

Quantum Energy Teleportation: A Novel Protocol Relaxing Previous Constraints

Songbo Xie,¹ Manas Sajjan,¹ and Sabre Kais^{1,*}

¹*Department of Electrical and Computer Engineering,
North Carolina State University, Raleigh, North Carolina 27606, USA*

(Dated: February 11, 2025)

Quantum state teleportation (QST) is a foundational protocol for transferring quantum information across long distances. Building on this concept, quantum energy teleportation (QET) was introduced to facilitate the transfer of energy. However, QET has traditionally been thought to impose much stricter constraints than QST, including the need for the initial state to be the ground state of a specific interacting Hamiltonian, for Alice’s measurement to commute with the interaction terms, and for the ground state to exhibit entanglement. These constraints limit broader application of the QET protocol. In this work, we challenge these notions and demonstrate for the first time that none of these constraints are fundamentally necessary. We propose a novel QET protocol that relaxes all these constraints, offering a more flexible and generalized framework. Additionally, we introduce the concept of a “local effective Hamiltonian,” which removes the need for optimization techniques in determining Bob’s optimal energy extraction. These advancements enhance our understanding of QET and extends its broader applications for quantum technologies. To support our findings, we implement the protocol on quantum hardware, confirming its theoretical validity and experimental feasibility.

I. INTRODUCTION

Quantum state teleportation (QST) is widely recognized for its ability to transfer quantum states to distant locations [1–3]. However, it is well understood that the energy associated with a quantum state cannot be teleported, as the sender transmits only information about the state. Using this information, along with classical communication and shared entanglement, the receiver reconstructs the quantum state. The energy required for this reconstruction is supplied locally by the receiver, rather than being teleported from the sender.

In contrast, a related protocol, quantum energy teleportation (QET), was believed to enable the teleportation of energy [4, 5]. Similar to QST, QET relies on classical communication to ensure that energy transfer does not exceed the speed of light. However, QET imposes stricter constraints compared to QST. While QST only requires the sender and receiver to share an entangled state, QET further requires that this state be the ground state of an interacting Hamiltonian. Additionally, in QST, the sender performs a measurement and transmits the outcome to the receiver via a classical communication channel. In QET, however, the observable used for the measurement must also commute with the interaction term in the Hamiltonian, ensuring that the local energy of the receiver remains undisturbed prior to the teleportation process.

Since its initial discovery in spin-chain systems [4, 6], QET has been extensively explored in many other physical systems. Theoretical studies have investigated its application in relativistic quantum field theory [7, 8], trapped ions [9], harmonic oscillators [10], black-hole physics [11], linear harmonic chains [12], quantum Hall systems [13], Gibbs spin particles [14, 15], squeezed vacuum states [16], topological orders [17], and quantum information science [18]. More recently, experimental efforts have demonstrated progress toward realizing QET, including in an NMR system [19] and on superconducting quantum hardware [20]. The combination of QST and QET was proposed to enable a long-range QET protocol [21]. A trade-off relationship between QST and QET was proposed, suggesting their potential exclusivity [22]. In [23], a relation between QET and quantum steering was suggested.

As research on QET has progressed, a deeper understanding of the protocol has been achieved. It has been argued that the energy extracted by the receiver is not physically transported from the sender. Instead, the sender’s classical message enables the receiver to access energy that was previously unavailable. This argument was supported in [24], where the receiver’s extracted energy can exceed the sender’s injected energy, indicating that the extracted energy cannot originate from the sender. In this sense, the QET protocol does not truly teleport energy but rather activates energy that was inaccessible to the receiver prior to the implementation of the protocol [19]. This inaccessibility of energy extraction is rigorously described by the concept of *strong local passive* (SLP) states [25, 26]. An SLP state is a multipartite quantum state, denoted by ρ , where no local quantum operation \mathcal{G}_B applied to a subsystem can

*Electronic address: skais@ncsu.edu

extract energy from the total system, characterized by the Hamiltonian H . Mathematically, this is expressed as the nonnegativity of the energy difference:

$$\Delta E = \text{Tr}[H(\mathcal{I}_A \otimes \mathcal{G}_B)\rho] - \text{Tr}(H\rho) \geq 0, \quad \forall \mathcal{G}_B. \quad (1)$$

In a QET protocol, the two parties share an SLP state, preventing the receiver from locally extracting energy. The sender then measures its local qubit, but the two-qubit system remains in an SLP state, meaning the receiver still cannot extract energy. However, classical communication between the sender and receiver breaks this limitation, making ΔE negative. A negative ΔE indicates that the receiver can locally extract energy, overcoming the restriction imposed by strong local passivity.

However, as has been noted, the QET protocol has traditionally been thought to impose strict constraints on the initial shared multipartite state and the observables employed by the sender during measurement. In this work, we challenge this notion and, for the first time, demonstrate that these constraints are not necessary. Specifically, we propose a novel QET protocol that relaxes these restrictions by introducing the concept of a local ‘‘effective Hamiltonian.’’ The relaxation of these constraints reveals that scenarios in which the energy within a system remains locally inaccessible are more frequent than previously believed. Additionally, the introduction of the local effective Hamiltonian simplifies the identification of optimal operations for the receiver to extract maximal energy, eliminating the need for cumbersome optimization techniques. Therefore, our results not only deepen the understanding of QET and its connection to SLP states but also expand its potential applications in quantum science and technology.

Finally, we validate our new protocol on quantum hardware, confirming both their theoretical correctness and experimental feasibility.

II. QUANTUM ENERGY TELEPORTATION AND LOCALLY INACCESSIBLE ENERGY

To begin, we revisit the minimal model of QET introduced in [27], which involves two qubits, A and B , shared between the sender (Alice) and the receiver (Bob). The Hamiltonian of the system is given by:

$$H_{AB} = -hZ_A - hZ_B + 2\kappa X_A \otimes X_B, \quad (2)$$

where h and κ are positive constants, and X_i and Z_i (with $i \in \{A, B\}$) are the Pauli- X and Pauli- Z operators for qubit i . The two qubits are initially prepared in the ground state $|g\rangle$ of H_{AB} , expressed as:

$$|g\rangle = \cos(\theta)|00\rangle_{AB} - \sin(\theta)|11\rangle_{AB}, \quad (3)$$

where $\tan(2\theta) \equiv \kappa/h$. Since the ground state has the lowest possible energy, neither Alice nor Bob can extract any energy from $|g\rangle$.

To enable energy extraction, the QET protocol requires Alice to measure her local qubit using the operators $\{|+\rangle\langle+|, |-\rangle\langle-|\}$, where $|\pm\rangle = (|0\rangle \pm |1\rangle)/\sqrt{2}$. These measurement operators commute with the interaction Hamiltonian:

$$[|+\rangle\langle+|, 2\kappa X_A \otimes X_B] = [|-\rangle\langle-|, 2\kappa X_A \otimes X_B] = 0.$$

This commutativity ensures that Alice’s measurement, while injecting energy into the two-qubit system and altering its state away from the ground state $|g\rangle$, does not disturb the terms associated with Bob’s subsystem. Specifically, the measurement only affects the expectation value of the $-hZ_A$ term in Eq. (2), which corresponds to Alice’s qubit. In contrast, the terms associated with Bob, $-hZ_B + 2\kappa X_A \otimes X_B$, remain unaffected, with their expectation values preserved as in the ground state $|g\rangle$. This guarantees that any energy extracted by Bob originates entirely from the previously inaccessible energy within the ground state $|g\rangle$, rather than from the energy injected by Alice.

Notably, after Alice’s measurement, the state of the system becomes:

$$\rho_{\text{SLP}} = \frac{1}{2} \left(|+\rangle\langle+|_A \otimes |b^+\rangle\langle b^+|_B + |-\rangle\langle-|_A \otimes |b^-\rangle\langle b^-|_B \right), \quad (4)$$

with $|b^\pm\rangle = \cos(\theta)|0\rangle \mp \sin(\theta)|1\rangle$ representing Bob’s local states after the measurement. The state ρ_{SLP} is an SLP state, meaning that Bob cannot extract energy from it using any local general operation \mathcal{G} , as explained earlier.

For Bob to access the inaccessible energy within Eq. (4), the QET protocol requires Alice to communicate her measurement outcome to Bob, based on which, Bob applies a conditional operator

$$G_\pm \equiv \exp[\pm i(\phi - \theta)Y], \quad (5)$$

to his qubit, where $\tan(2\phi) \equiv 2\kappa/h$, with the sign \pm depending on Alice's measurement outcome. Y is the Pauli- Y operator. The resulting state, expressed as:

$$\rho_f = \frac{1}{2} \left[|+\rangle\langle +|_A \otimes \left(G_+ |b^+\rangle\langle b^+|_B G_+^\dagger \right) + |-\rangle\langle -|_A \otimes \left(G_- |b^-\rangle\langle b^-|_B G_-^\dagger \right) \right], \quad (6)$$

exhibits a negative energy difference:

$$\Delta E = \text{Tr}(H_{AB}\rho_f) - \text{Tr}(H_{AB}\rho_{\text{SLP}}) = -2h \sin^2(\phi - \theta) < 0. \quad (7)$$

This negativity indicates that Bob's conditional operation successfully breaks the limit of strong local passivity, allowing him to extract the previously inaccessible energy that would remain unavailable without Alice's classical communication.

Since the initial discovery of QET, the joint system has always been prepared in the ground state $|g\rangle$ of a given Hamiltonian, corresponding to the lowest possible energy configuration where both Alice's and Bob's qubits have minimal energy. When Alice measures her qubit, energy is injected into the system, deviating the state from $|g\rangle$. However, this energy remains localized to Alice's subsystem because the measurement observable commutes with the interaction Hamiltonian. As a result, Bob's local energy remains unchanged at its minimum value, preventing him from extracting energy immediately after Alice's measurement.

Once Alice communicates her measurement outcome to Bob, he performs the conditional operation G_\pm to extract energy. Since Bob's local energy is kept at its minimum, the energy he extracts was believed to be transported from the energy injected by Alice during her measurement. This understanding gives rise to the term "quantum energy teleportation" (QET). Importantly, QET requires classical communication between Alice and Bob, ensuring that energy transfer does not exceed the speed of light, thus preserving causality [28]. This is conceptually analogous to QST, where classical communication similarly ensures causality, preventing superluminal transfer of quantum information.

However, it was later realized that this interpretation of QET was incorrect [19]. In fact, energy is not transported during the QET process. Although $|g\rangle$ is the ground state of the total Hamiltonian H_{AB} , it is not the ground state of the partial Hamiltonian, $-\hbar Z_B + 2\kappa X_A \otimes X_B$, obtained by excluding terms that do not involve Bob. This means that there is potential for Bob to extract energy from the system by locally driving his qubit to the ground state of this partial Hamiltonian. However, this extraction is prevented because the joint state remains an SLP state both before and after Alice's measurement. In this framework, the classical communication in the QET protocol does not physically transfer energy but instead enables Bob to unlock and access the previously inaccessible energy stored within his subsystem [24]. The conclusion that no energy is transferred during QET can be further confirmed by the fact that Alice's local energy, the expectation value of $-\hbar Z_A$, remains unaffected by Bob's conditional operations.

Although QET has been discussed in a close association with SLP states, the protocol remains widely misunderstood. To date, three constraints have been considered necessary for any QET protocol, but we demonstrate that none of these conditions are strictly required:

- (a) **Ground State:** It has been argued that if a density matrix ρ commutes with the Hamiltonian, $[\rho, H_{AB}] = 0$, and the population of the ground state $|g\rangle$ exceeds a threshold p^* (as defined in [25]), then ρ is an SLP state. Consequently, all existing QET protocols initialize the system in the ground state $|g\rangle$ of H_{AB} , ensuring the state after Alice's measurement retains sufficient population in $|g\rangle$ to preserve the SLP property. However, this condition is only sufficient, not necessary. We show that QET protocols can function even when the system begins in an excited pure state with zero population in $|g\rangle$. After Alice's measurement, the resulting state can still be an SLP state, requiring Bob to rely on Alice's information for energy extraction.
- (b) **Commutativity:** It is widely assumed that the observable used by Alice for her measurement must commute with the interaction term in H_{AB} to prevent her measurement from injecting energy into Bob's surroundings, hence preserving the SLP property. However, this condition is not strictly necessary. We show that even when Alice's measurement observable does not commute with the interaction term, the interaction Hamiltonian can remain unaffected. Additionally, the resulting state still retains its SLP property.
- (c) **Entanglement:** Finally, it is believed that the shared state between Alice and Bob must be entangled for Alice's measurement to have any influence on Bob's subsystem. Relations were studied between the entanglement breaking due to Alice's measurement and teleported energy [27]. Arguments also suggested that if the ground state is entangled and Alice's measurement disentangles the system, it becomes impossible for Bob, using only local operations and classical communications, to restore the entangled ground state and extract energy [26]. Along the same line, it was also suggested that quantum resources can improve the energy extraction efficiency for QET [29]. However, we demonstrate that entanglement is not a strict requirement for QET. By introducing

the concept of a *local effective Hamiltonian*, we show that Alice's actions can influence Bob's subsystem not only by changing the "departure state" through entanglement but also by changing the "destination state" via the effective Hamiltonian. Thus, the requirement of entanglement can be relaxed.

III. A QET PROTOCOL RELAXING ALL THREE CONSTRAINTS

We propose a new QET protocol involving two qubits, A and B , shared between Alice and Bob, under the following flip-flop Hamiltonian:

$$\begin{aligned} H_{AB} &= -hZ_A - hZ_B + 2\kappa(\sigma_+ \otimes \sigma_- + \sigma_- \otimes \sigma_+) \\ &\equiv -hZ_A - hZ_B + \kappa(X_A \otimes X_B + Y_A \otimes Y_B), \end{aligned} \quad (8)$$

where Z , X , and Y represent the Pauli matrices, and $\sigma_{\pm} \equiv (X \mp iY)/2$ are the qubit raising and lowering operators.

Compared to Eq. (2), this Hamiltonian includes an additional $Y_A \otimes Y_B$ interaction term. Consequently, the total interaction term, $(X_A \otimes X_B + Y_A \otimes Y_B)$, cannot be factorized.

We consider the deep strong coupling regime [30], setting $\kappa > h > 0$. In this regime, the Hamiltonian in Eq. (8) has four eigenstates with corresponding eigenvalues:

$$\begin{aligned} (|01\rangle - |10\rangle)/\sqrt{2}, & \quad -2\kappa, \\ |00\rangle, & \quad -2h, \\ |11\rangle, & \quad +2h, \\ (|01\rangle + |10\rangle)/\sqrt{2}, & \quad +2\kappa. \end{aligned} \quad (9)$$

We choose the first excited state, $|00\rangle$, as the initial state. Alice then measures her qubit A using the operators $\{|+\rangle\langle+|, |-\rangle\langle-|\}$. Regardless of the outcome, Bob's qubit remains in state $|0\rangle$, as the qubits are disentangled. The density matrix after Alice's measurement is

$$\rho_{\text{SLP}} = \frac{1}{2} (|0\rangle\langle 0|_A \otimes |0\rangle\langle 0|_B + |1\rangle\langle 1|_A \otimes |0\rangle\langle 0|_B). \quad (10)$$

To verify whether this state is SLP for Bob according to the Hamiltonian Eq. (8), one would need to check the inequality in Eq. (1), which involves parameterizing Bob's general operation with 12 parameters for a qubit completely positive trace-preserving (CPTP) map [31–34]. However, a necessary and sufficient condition for determining whether a state ρ is SLP for a Hamiltonian H is given by a 4×4 matrix $M(\rho, H)$, the form of which is defined in [26] and given in Appendix A. Specifically, ρ is SLP for H if and only if $M(\rho, H)$ is positive semi-definite.

In our case, it is straightforward to verify that both $M(|00\rangle\langle 00|, H_{AB})$ and $M(\rho_{\text{SLP}}, H_{AB})$ share the identical eigenvalue set, $\{2, 0, 0, 0\}$, all of which are nonnegative, confirming that these two matrices are positive semi-definite. Thus, starting from the first excited state $|00\rangle$, Bob cannot extract energy locally. After Alice's measurement, the state evolves to Eq. (10), and Bob still cannot extract energy locally. Instead, Bob needs communication from Alice for his energy extraction.

In contrast, if we had started with any of the other three eigenstates in Eq. (9), including the ground state $(|01\rangle - |10\rangle)/\sqrt{2}$, the resulting states after Alice's measurement would not maintain the SLP property. Specifically, starting from the ground state, and performing Alice's measurement, we compute the M matrix of the resulting state and find its four eigenvalues to be $\{2, 1.5, -0.5, 0\}$. This confirms that the post-measurement state is not an SLP state, meaning QET protocols are not necessary for Bob's energy extraction. Therefore, our initial choice of the first excited state $|00\rangle$ is well justified.

Through the new protocol, we observe that all three previously considered constraints for QET are relaxed. First, the system is initialized in an excited state where the ground-state population is zero. Second, although Alice's measurement does not commute with the interaction term $Y_A \otimes Y_B$, it does not inject energy to this term, as $\langle Y_A \otimes Y_B \rangle$ remains 0 throughout the entire process. Finally, the system begins in the product state $|00\rangle$, meaning Alice's measurement cannot directly affect Bob's local state. However, for Bob to extract energy based on Alice's measurement outcome, her action must influence Bob's subsystem. To address this, we introduce the concept of a *local effective Hamiltonian* for Bob and show that Alice's measurement modifies Bob's local effective Hamiltonian rather than his local state.

Since the two qubits remain disentangled after Alice's measurement, the total energy of the system is given by

$$\langle H_{AB} \rangle = -h\langle Z_A \rangle_A - h\langle Z_B \rangle_B + \kappa\langle X_A \rangle_A \langle X_B \rangle_B + \kappa\langle Y_A \rangle_A \langle Y_B \rangle_B, \quad (11)$$

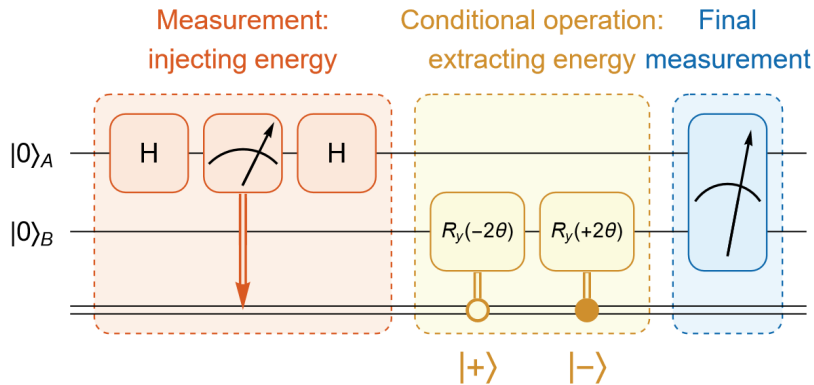


FIG. 1: The quantum circuit implemented on IBM quantum hardware for verifying the feasibility of our proposed QET protocol. Since the system begins in the first excited state of the Hamiltonian in Eq. (8), $|0\rangle \otimes |0\rangle$, no additional state preparation is required. Alice initiates the protocol by performing a measurement, which injects energy into the system. After receiving Alice’s measurement outcome, Bob applies a conditional operation to extract energy from the system. A final measurement is then performed to verify the energy distribution within the system.

where $\langle \cdot \rangle_A \equiv \langle \psi_A | \cdot | \psi_A \rangle$ denotes the expectation value of the operator \cdot with respect to Alice’s state $|\psi_A\rangle$, and similar for $\langle \cdot \rangle_B$ with respect to Bob’s state.

If Alice’s measurement yields the outcome $+$, her state collapses to $|+\rangle$, and the total energy becomes

$$\langle H_{AB} \rangle = -\hbar \langle Z_B \rangle_B + \kappa \langle X_B \rangle_B, \quad (12)$$

implying that Bob’s effective Hamiltonian is $-\hbar Z_B + \kappa X_B$. Similarly, if Alice’s outcome is $-$, Bob’s effective Hamiltonian becomes $-\hbar Z_B - \kappa X_B$.

One might wonder whether this effective Hamiltonian has a dynamical effect on Bob’s qubit. The answer is yes. To show this, Alice fixes her state after the measurement using the quantum Zeno effect [35–37], by repeatedly measuring her state at a rate much faster than the timescale of H_{AB} , which is commonly characterized by $\max(\hbar, \kappa)$.

By assuming that Alice’s measurement outcome is $+$ (the analysis for $-$ follows similarly), the general two-qubit state is given by:

$$|\psi(t)\rangle = |+\rangle_A \otimes |\varphi(t)\rangle_B. \quad (13)$$

Under Schrödinger’s equation, the time evolution of the state is:

$$|\psi(t+dt)\rangle = \left(|+\rangle\langle +| \otimes \mathbb{I} \right) \left(\mathbb{I} - iH_{AB}dt \right) |\psi(t)\rangle, \quad (14)$$

where the second term represents free evolution under H_{AB} , and the first term enforces the projective operator due to Alice’s repeated measurements.

Using $\langle +|X|+\rangle = 1$ and $\langle +|Y|+\rangle = \langle +|Z|+\rangle = 0$, the evolution simplifies to:

$$|\varphi(t+dt)\rangle = \left(\mathbb{I} - i(-\hbar Z_B + \kappa X_B)dt \right) |\varphi(t)\rangle, \quad (15)$$

or equivalently:

$$i \frac{\partial}{\partial t} |\varphi(t)\rangle = \left(-\hbar Z_B + \kappa X_B \right) |\varphi(t)\rangle. \quad (16)$$

Similarly, for the $-$ outcome, Bob’s effective Hamiltonian becomes $-\hbar Z_B - \kappa X_B$. Thus, the local effective Hamiltonian for Bob is:

$$H_B^{(\pm)} = -\hbar Z_B \pm \kappa X_B. \quad (17)$$

For Bob to extract energy using Alice’s information, we diagonalize the effective Hamiltonian Eq. (17). The ground states $|g^\pm\rangle$ and excited states $|e^\pm\rangle$ of the effective Hamiltonian, together with their eigenvalues, are given by:

$$\begin{aligned} -\sqrt{\hbar^2 + \kappa^2}, \quad |g^\pm\rangle &\equiv \cos(\theta)|0\rangle \mp \sin(\theta)|1\rangle, \\ +\sqrt{\hbar^2 + \kappa^2}, \quad |e^\pm\rangle &\equiv \pm \sin(\theta)|0\rangle + \cos(\theta)|1\rangle. \end{aligned} \quad (18)$$

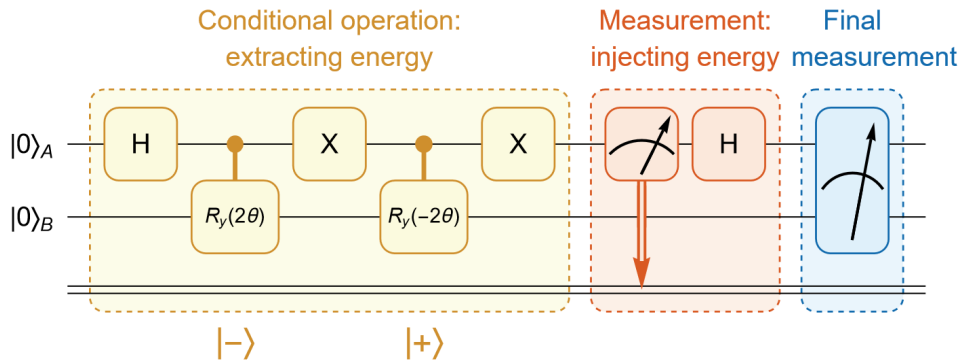


FIG. 2: To address the current lack of support for dynamic circuits by IBM quantum hardware, we use an alternative but equivalent circuit. In this approach, Alice’s measurement is postponed until after Bob’s conditional operations, and Bob’s conditional operations are replaced with two-qubit controlled operations. It can be shown that the two circuits are equivalent, as they yield identical resulting density matrices.

where $\tan(2\theta) = \kappa/h$. The effective Hamiltonian can be reformulated as

$$H_B^{(\pm)} = \sqrt{h^2 + \kappa^2} \left(|e^\pm\rangle\langle e^\pm| - |g^\pm\rangle\langle g^\pm| \right). \quad (19)$$

We now highlight an additional advantage of introducing the local effective Hamiltonian (17). In general QET protocols, determining Bob’s optimal conditional operations for maximal energy extraction required cumbersome optimization techniques, typically involving the parameterization of a general single-qubit unitary operation (for example, see [38]). However, once the conditional Hamiltonian is established, Bob’s optimal operations simply correspond to unitary transformations that rotate his current state to the conditional ground states $|g^\pm\rangle$ of the effective Hamiltonians.

Specifically, in our case, to extract energy, Bob applies to his qubit the conditional RY gate, $RY(\mp 2\theta) = \exp(\pm 2i\theta Y)$, which rotates his initial state $|0\rangle \equiv \cos(\theta) \pm \sin(\theta)|1\rangle$ to the corresponding ground state $|g^\pm\rangle$. This highlights the role of the effective Hamiltonian: although Alice and Bob are initially unentangled, Alice’s measurement influences Bob by modifying his destination state via the effective Hamiltonian. Thus, entanglement is not required in this QET protocol. As can be verified, the amount of energy that Bob extracts is:

$$E_{\text{extract}} = 2 \sin^2(\theta) \sqrt{h^2 + \kappa^2}. \quad (20)$$

IV. EXPERIMENTAL VERIFICATION OF QET PROTOCOL ON QUANTUM HARDWARE

To validate the feasibility of our proposed QET protocol and demonstrate that the three traditional constraints are unnecessary, we implement the protocol on IBM quantum hardware. The quantum circuit used for this implementation is shown in Fig. 1, which includes mid-circuit measurements, often referred to as dynamic circuits.

Recently, IBM hardware has removed its support of dynamic circuits. To address this limitation, we adopt the approach introduced in [20], replacing Bob’s conditional operations with two-qubit controlled operations while delaying Alice’s measurement until after these controlled operations. It can be shown that the two approaches are equivalent in the sense that they produce the same final density matrix.

To show this, suppose Bob’s operation is $U(\pm)$, conditional on Alice’s measurement outcome \pm . After Alice’s measurement and Bob’s operation, the state becomes:

$$\rho \rightarrow \left(|+\rangle\langle +| \otimes U(+)\right) \rho \left(|+\rangle\langle +| \otimes U^\dagger(+)\right) + \left(|-\rangle\langle -| \otimes U(-)\right) \rho \left(|-\rangle\langle -| \otimes U^\dagger(-)\right). \quad (21)$$

Alternatively, in the modified quantum circuit, the two-qubit controlled unitary operations are applied first. The state is firstly transformed as:

$$\rho \rightarrow \left(|+\rangle\langle +| \otimes U(+)\right) + \left(|-\rangle\langle -| \otimes U(-)\right) \rho \left(|+\rangle\langle +| \otimes U^\dagger(+)\right) + \left(|-\rangle\langle -| \otimes U^\dagger(-)\right). \quad (22)$$

After this transformation, Alice performs her delayed measurement. This measurement projects the state in Eq. (22) into the same final state as Eq. (21), showing the equivalence of the two approaches.

In our case, the original quantum circuit for our protocol is shown in Fig. 1, where the initial state is $|0\rangle_A \otimes |0\rangle_B$. The red block represents Alice’s measurement in the basis $\{|+\rangle, |-\rangle\}$. The yellow block represents Bob’s conditional operation based on Alice’s classical information. The blue block corresponds to the final measurement used to check the energy.

Instead, we replace the original circuit with the modified version shown in Fig. 2. In this circuit, the yellow block is firstly implemented which corresponds to Bob’s controlled operation based on Alice’s quantum state in her computational basis. The red block now represents Alice’s delayed measurement. The two circuits are equivalent as they yield the same final density matrix and identical measurement outcomes for any observables.

For choice of the parameters, without loss of generality, we choose $h = 1$. Then we choose $\kappa = 1.5$, which satisfies the relation $\kappa > h$. By substituting these into Eq. (20), we have the analytical value of the extracted energy $E_{\text{extract}} = 0.8028$.

Next, for the number of shots, we use 20,000 shots for each observable measurement, as can be justified by applying Chebyshev’s inequality:

$$P(|\bar{\mathcal{O}} - \langle \mathcal{O} \rangle| \geq \varepsilon) \leq \frac{\text{Var}(\mathcal{O})}{N\varepsilon^2} \leq \delta, \quad (23)$$

where $\bar{\mathcal{O}}$ is the statistical mean obtained from the measurements of an arbitrary observable \mathcal{O} , and $\langle \mathcal{O} \rangle$ is its theoretical expectation value. In our case, \mathcal{O} is always a Pauli word (product of individual Pauli operators), so $\text{Var}(\mathcal{O})$ is upper bounded by 1. This gives the relation $\delta \geq 1/(N\varepsilon^2)$.

For $N = 20,000$, if we set $\varepsilon = 0.02$, we find $\delta = 1/8$. This implies there is at most a 1/8 probability that our measurement outcome deviates from the true value by more than 0.02. This level of accuracy is sufficient for our experimental purposes.

For the backends, we choose three available IBM hardware backends: `ibm_brussels`, `ibm_kyiv`, and `ibm_torino`. Detailed specifications for these backends, along with their qubit distribution maps, are provided in Appendix B. Additionally, we execute the circuits using the `AerSimulator`, a classical simulator capable of running quantum circuits locally on personal computers. When no noise is introduced, the `AerSimulator` is expected to produce exact results, serving as a benchmark for the design of the quantum circuits.

Backend	Operator	Result	Backend	Operator	Result
Analytical		1.0	Analytical		0.5547
AerSimulator		1.0	AerSimulator		0.5547
ibm_brussels	$\langle \mathbb{I}_A \otimes Z_B \rangle$	1.0081 ± 0.0072	ibm_brussels	$\langle \mathbb{I}_A \otimes Z_B \rangle$	0.5461 ± 0.0068
ibm_kyiv		1.0035 ± 0.0034	ibm_kyiv		0.5217 ± 0.0060
ibm_torino		1.1015 ± 0.0195	ibm_torino		0.6515 ± 0.6515
Analytical		0.0	Analytical		-0.8320
AerSimulator		0.0	AerSimulator		-0.8320
ibm_brussels	$\langle X_A \otimes X_B \rangle$	0.0029 ± 0.0073	ibm_brussels	$\langle X_A \otimes X_B \rangle$	-0.6361 ± 0.0085
ibm_kyiv		0.0121 ± 0.0064	ibm_kyiv		-0.7697 ± 0.0043
ibm_torino		-0.0062 ± 0.0106	ibm_torino		-0.8495 ± -0.8495
Analytical		0.0	Analytical		0.0
AerSimulator		0.0	AerSimulator		0.0
ibm_brussels	$\langle Y_A \otimes Y_B \rangle$	0.0185 ± 0.0083	ibm_brussels	$\langle Y_A \otimes Y_B \rangle$	0.0069 ± 0.0072
ibm_kyiv		0.0001 ± 0.0060	ibm_kyiv		-0.0129 ± 0.0074
ibm_torino		0.0153 ± 0.0095	ibm_torino		0.0105 ± 0.0105
Analytical		-1.0	Analytical		-1.8028
AerSimulator		-1.0	AerSimulator		-1.8028
ibm_brussels	$\langle E_{\text{Bob}} \rangle$	-0.9760 ± 0.0161	ibm_brussels	$\langle E_{\text{Bob}} \rangle$	-1.4899 ± 0.0168
ibm_kyiv		-0.9852 ± 0.0152	ibm_kyiv		-1.6956 ± 0.0115
ibm_torino		-1.0878 ± 0.0107	ibm_torino		-1.9100 ± 0.0364

TABLE I: The measurement results for the QET protocol are presented in two tables. The left table shows the results obtained before Bob’s conditional operations, which corresponds to removing the yellow block in Fig. 1 while retaining the rest of the circuit. The right table shows the results after Bob’s conditional operations, corresponding exactly to the circuit shown in Fig. 2. Three operators are measured: $\mathbb{I}_A \otimes Z_B$, $X_A \otimes X_B$, and $Y_A \otimes Y_B$, yielding the final value of E_{Bob} , representing Bob’s energy. The difference between the results in the two tables signifies the energy extracted by Bob’s conditional operations, as are further given in Table II.

The measurement results are listed in Table I. In the left table, we report the measurements of the three operators

$\mathbb{I}_A \otimes Z_B$, $X_A \otimes X_B$, and $Y_A \otimes Y_B$ prior to Bob applying his conditional operations. In the right table, these operators are measured after Bob has applied his conditional operations. The energy that we are interested in is given by:

$$E_{\text{Bob}} = -h\langle \mathbb{I}_A \otimes Z_B \rangle + \kappa\langle X_A \otimes X_B \rangle + \kappa\langle Y_A \otimes Y_B \rangle. \quad (24)$$

The term $-h\langle Z_A \otimes \mathbb{I}_B \rangle$ is omitted from our calculation, as it remains unaffected by Bob’s conditional operations. E_{Bob} is compared before and after Bob’s conditional operations. If the energy in the right table is smaller than that in the left table, it indicates that Bob’s conditional operation has successfully extracted energy from the system.

The standard deviations in these measurements arise only from statistical fluctuations and do not account for systematic errors introduced by the near-term intermediate-scale quantum (NISQ) nature of IBM hardware. To minimize systematic errors, we use the measurement error mitigation technique [39], implemented as a built-in function within IBM’s `qiskit` package, by setting the resilience level to 1. This approach effectively reduces errors occurring during the measurement process of the quantum circuit. These corrections are directly incorporated into the expectation values of each measurement outcome, while the standard deviations only reflect statistical uncertainty.

Backends	Analytical	AerSimulator	ibm_brussels	ibm_kyiv	ibm_torino
Extracted energy	0.8028	0.8028	0.5139 ± 0.0233	0.7104 ± 0.0191	0.8222 ± 0.0379

TABLE II: The energy extracted by Bob is presented for the three IBM quantum hardware backends, along with results from the AerSimulator and the analytical solution. All three quantum hardware backends successfully extract energy from the system, thereby breaking the restriction of strong local passivity and confirming the feasibility of our proposed QET protocol.

By comparing the results in the two panels, the extracted energy can be calculated and is presented in Table II. The standard deviation for the extracted energy is determined using the error propagation formula. Specifically, since $E_{\text{extract}} = E_{\text{Bob}}^{\text{left}} - E_{\text{Bob}}^{\text{right}}$, the standard deviation is given by $\Delta E_{\text{extract}} = \sqrt{(\Delta E_{\text{Bob}}^{\text{left}})^2 + (\Delta E_{\text{Bob}}^{\text{right}})^2}$. Notably, the `ibm_torino` backend produced results closer to the analytical solution compared to the other two backends. This improvement is attributed to the newer Heron processor used by `ibm_torino`, whereas the other two backends use Eagle processors. Further details about these processors are provided in Appendix B.

The results demonstrate that all three quantum hardware backends successfully provide positive extracted energy. This confirms the experimental feasibility of our newly proposed QET protocol and further establishes the fact that the three previously considered constraints for QET are unnecessary.

V. SUMMARY

Quantum state teleportation (QST) is a well-established protocol for transferring quantum states between distant locations. However, the energy required to reconstruct the quantum state is provided by the receiver (Bob), rather than being transmitted directly from the sender (Alice). As a result, QST is not capable of teleporting energy. In contrast, the quantum energy teleportation (QET) protocol was introduced in the purpose of enabling energy transfer between distant locations. However, unlike QST, QET imposes significantly stricter constraints. These include the need for the initial state shared by Alice and Bob to be entangled and to correspond to the ground state of an interacting Hamiltonian. Additionally, the observable used by Alice for her measurement must commute with the interaction term in the Hamiltonian. While these conditions initially appear reasonable for implementing QET, they are overly restrictive and limit the broader applicability of the protocol.

Recent advancements in the understanding of the QET protocol have revealed that no energy is actually teleported from Alice to Bob within the protocol. Instead, Alice’s message acts as a key that enables Bob to access and extract his local energy, which was previously inaccessible. In light of this insight, the previously considered “reasonable” constraints for QET, which are mentioned above, appear less justified. Nevertheless, these strict conditions are still widely regarded as essential for implementing a QET protocol.

In this work, we introduce a new QET protocol which, for the first time, removes the three previously considered essential constraints. Specifically, Alice and Bob begin with a product state, which corresponds to an excited eigenstate of the Hamiltonian rather than its ground state. Furthermore, Alice’s measurement does not commute with the interaction term of the Hamiltonian. Despite this, we demonstrate that the system maintains the property of strong local passivity both before and after Alice’s measurement. This ensures that Bob cannot locally extract energy from the system. Instead, Alice communicates her measurement outcome to Bob, enabling him to perform conditional operations. These conditional operations allow Bob to extract energy, effectively performing the QET protocol while removing all three constraints.

Furthermore, we implement our new QET protocol on three available IBM quantum hardware backends. The results from all three backends demonstrate positive extracted energy for Bob, validating the feasibility of our protocol in experimental settings and confirming that the three previously considered constraints are not necessary. These successful implementations confirm the effectiveness of our new protocol, providing deeper insights into quantum energy teleportation and enabling its broader applications by removing unnecessary constraints.

Our results suggest that the phenomenon of locked energy due to strong local passivity extends beyond the systems initially anticipated by researchers. These locked energies, which cannot be easily extracted, limit our ability to leverage them for practical applications. However, our newly proposed QET protocol provides a way to unlock and extract these otherwise inaccessible energies, making them available for future use. Potential future directions for this work include investigating the practical applications of these extracted energies in various quantum systems, such as in quantum chemistry, where energy extraction could enable new modeling of chemical reactions. Exploring these avenues could lead to significant advancements in both fundamental science and applied technologies.

As a separate remark, we recently noticed a similar study [38] that explores QET using the same Hamiltonian, Eq. (8), as ours. In their analysis, the entangled ground state $(|01\rangle - |10\rangle)/\sqrt{2}$ was chosen as the system's initial state. However, as discussed earlier, the post-measurement state derived from this ground state does not exhibit the SLP property, making QET protocols unnecessary for Bob's energy extraction. Instead, the excited state $|00\rangle$ must be used to apply QET. Furthermore, since their approach does not incorporate local effective Hamiltonians, they rely on optimization methods to determine Bob's unitary operations for optimal energy extraction. This further highlights the advantages of our results.

VI. ACKNOWLEDGMENTS

We would like to thank Professor Joseph H. Eberly and Professor Peter W. Milonni for valuable discussions. We acknowledge funding from the Office of Science through the Quantum Science Center (QSC), a National Quantum Information Science Research Center.

-
- [1] C. H. Bennett, G. Brassard, C. Crépeau, R. Jozsa, A. Peres, and W. K. Wootters, *Phys. Rev. Lett.* **70**, 1895 (1993).
 - [2] D. Bouwmeester, J.-W. Pan, K. Mattle, M. Eibl, H. Weinfurter, and A. Zeilinger, *Nature* **390**, 575 (1997).
 - [3] A. Furusawa, J. L. Sørensen, S. L. Braunstein, C. A. Fuchs, H. J. Kimble, and E. S. Polzik, *Science* **282**, 706 (1998).
 - [4] M. Hotta, *J. Phys. Soc. Jpn.* **78**, 034001 (2009).
 - [5] M. Hotta, arXiv:1101.3954 .
 - [6] M. Hotta, *Phys. Lett. A* **372**, 5671 (2008).
 - [7] M. Hotta, *Phys. Rev. D* **78**, 045006 (2008).
 - [8] K. Ikeda, *Phys. Rev. D* **107**, L071502 (2023).
 - [9] M. Hotta, *Phys. Rev. A* **80**, 042323 (2009).
 - [10] M. Hotta, *J. Phys. A: Math. Theor.* **43**, 105305 (2010).
 - [11] M. Hotta, *Phys. Rev. D* **81**, 044025 (2010).
 - [12] Y. Nambu and M. Hotta, *Phys. Rev. A* **82**, 042329 (2010).
 - [13] G. Yusa, W. Izumida, and M. Hotta, *Phys. Rev. A* **84**, 032336 (2011).
 - [14] M. R. Frey, K. Gerlach, and M. Hotta, *J. Phys. A: Math. Theor.* **46**, 455304 (2013).
 - [15] J. Trevison and M. Hotta, *J. Phys. A: Math. Theor.* **48**, 175302 (2015).
 - [16] M. Hotta, J. Matsumoto, and G. Yusa, *Phys. Rev. A* **89**, 012311 (2014).
 - [17] K. Ikeda, *AVS Quantum Science* **5** (2023).
 - [18] K. Ikeda and A. Lowe, *Quantum Information Processing* **23**, 236 (2024).
 - [19] N. A. Rodríguez-Briones, H. Katiyar, E. Martín-Martínez, and R. Laflamme, *Phys. Rev. Lett.* **130**, 110801 (2023).
 - [20] K. Ikeda, *Phys. Rev. Applied* **20**, 024051 (2023).
 - [21] K. Ikeda, *IET Quantum Communication* (2023).
 - [22] J. Wang and S. Yao, arXiv:2405.13886 (2024).
 - [23] H. Fan, F.-L. Wu, L. Wang, S.-Q. Liu, and S.-Y. Liu, *Phys. Rev. A* **110**, 052424 (2024).
 - [24] F.-L. Wu, H. Fan, L. Wang, S.-Q. Liu, S.-Y. Liu, and W.-L. Yang, *Phys. Rev. A* **109**, 062208 (2024).
 - [25] M. Frey, K. Funo, and M. Hotta, *Phys. Rev. E* **90**, 012127 (2014).
 - [26] Á. M. Alhambra, G. Styliaris, N. A. Rodríguez-Briones, J. Sikora, and E. Martín-Martínez, *Phys. Rev. Lett.* **123**, 190601 (2019).
 - [27] M. Hotta, *Phys. Lett. A* **374**, 3416 (2010).
 - [28] G. Diener, *Phys. Lett. A* **235**, 118 (1997).
 - [29] H. Fan, F.-L. Wu, L. Wang, S.-Q. Liu, and S.-Y. Liu, *Quantum Information Processing* **23**, 367 (2024).
 - [30] P. Forn-Díaz, L. Lamata, E. Rico, J. Kono, and E. Solano, *Rev. Mod. Phys.* **91**, 025005 (2019).

- [31] M. A. Nielsen and I. L. Chuang, *Quantum computation and quantum information* (Cambridge university press, 2010).
- [32] S. Boyd and L. Vandenberghe, *Convex optimization* (Cambridge university press, 2004).
- [33] J. Watrous, *The theory of quantum information* (Cambridge university press, 2018).
- [34] J. Y. Sim, J. Suzuki, B.-G. Englert, and H. K. Ng, *Phys. Rev. A* **101**, 022307 (2020).
- [35] B. Misra and E. G. Sudarshan, *J. Math. Phys.* **18**, 756 (1977).
- [36] W. M. Itano, D. J. Heinzen, J. J. Bollinger, and D. J. Wineland, *Phys. Rev. A* **41**, 2295 (1990).
- [37] M. C. Fischer, B. Gutiérrez-Medina, and M. G. Raizen, *Phys. Rev. Lett.* **87**, 040402 (2001).
- [38] T. Haque, arXiv:2411.08927 (2024).
- [39] IBM Quantum, (2025), <https://quantum-computing.ibm.com/>.

Appendix A: Analytical Form of the Matrix $M(\rho, H)$

This is a repetition of the main result given in [26]. Given a Hamiltonian H_{AB} and a two-party state ρ_{AB} , we define the energy difference under a local completely positive trace-preserving (CPTP) map acting on subsystem B as:

$$\Delta E_{A(B)} = \min_{\mathcal{G}_B} \text{Tr}[H_{AB}(\mathcal{I}_A \otimes \mathcal{G}_B)\rho_{AB}] - \text{Tr}(H_{AB}\rho_{AB}).$$

It is easy to check that, the pair $\{\rho_{AB}, H_{AB}\}$ is strong local passive (SLP) with respect to subsystem B if and only if this energy difference vanishes:

$$\Delta E_{A(B)} = 0.$$

Now, consider an auxiliary Hilbert space B' with the same dimension as B . Define the Hermitian operator $C_{BB'} \in \mathcal{H}_B \otimes \mathcal{H}_{B'}$ as:

$$C_{BB'} = \text{Tr}_A \left[\rho_{AB}^{\Gamma_B} H_{AB'} \right],$$

where $\rho_{AB}^{\Gamma_B}$ denotes the partial transpose of ρ_{AB} on subsystem B . The Choi-Jamiołkowski operator for the identity channel is given by:

$$\mathcal{J}_{BB'}^{\mathcal{I}} \equiv 2|\Phi^+\rangle_{BB'}\langle\Phi^+|_{BB'} = (|0\rangle_B|0\rangle_{B'} + |1\rangle_B|1\rangle_{B'}) (\langle 0|_B\langle 0|_{B'} + \langle 1|_B\langle 1|_{B'}).$$

Finally, it is concluded that $\Delta E_{A(B)} = 0$ if and only if the Hermitian operator

$$M(\rho_{AB}, H_{AB}) \equiv C_{BB'} - \text{Tr}_{B'} [\mathcal{J}_{BB'}^{\mathcal{I}} C_{BB'}] \otimes \mathbb{I}_{B'}$$

is positive semidefinite, i.e.,

$$M(\rho_{AB}, H_{AB}) \geq 0.$$

Or equivalently, all its four eigenvalues are nonnegative. The proof of this result can be found in [26].

Appendix B: Details of the Quantum Hardware

The details of the three IBM quantum hardware backends are provided in this section. The qubit distribution maps for `ibm_brussels` and `ibm_kyiv` are shown in Fig. 3, while the map for `ibm_torino` is presented in Fig. 4. In all three quantum circuits, qubit 0 is used for Alice's qubit, and qubit 1 is used for Bob's qubit.

Table III provides detailed information about the three IBM quantum hardware backends, including the properties of the qubits used and the properties of the single-qubit and two-qubit gates employed in the experiments. This information was retrieved from [39] on January 13, 2025, the day when the quantum circuits were executed on these backends.

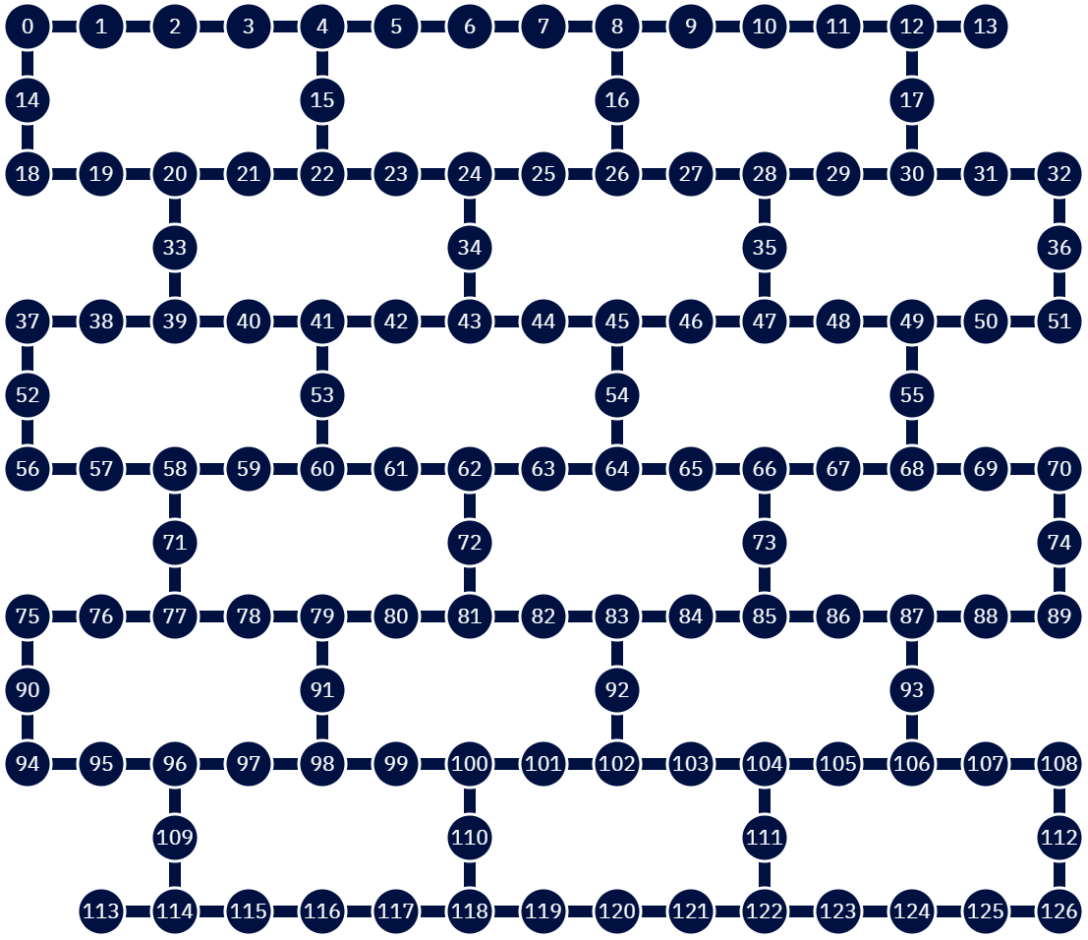


FIG. 3: Qubit distribution map for the backends of `ibm_brussels` and `ibm_kyiv` is demonstrated. Qubit 0 is used for Alice's qubit, and qubit 1 is used for Bob's qubit.

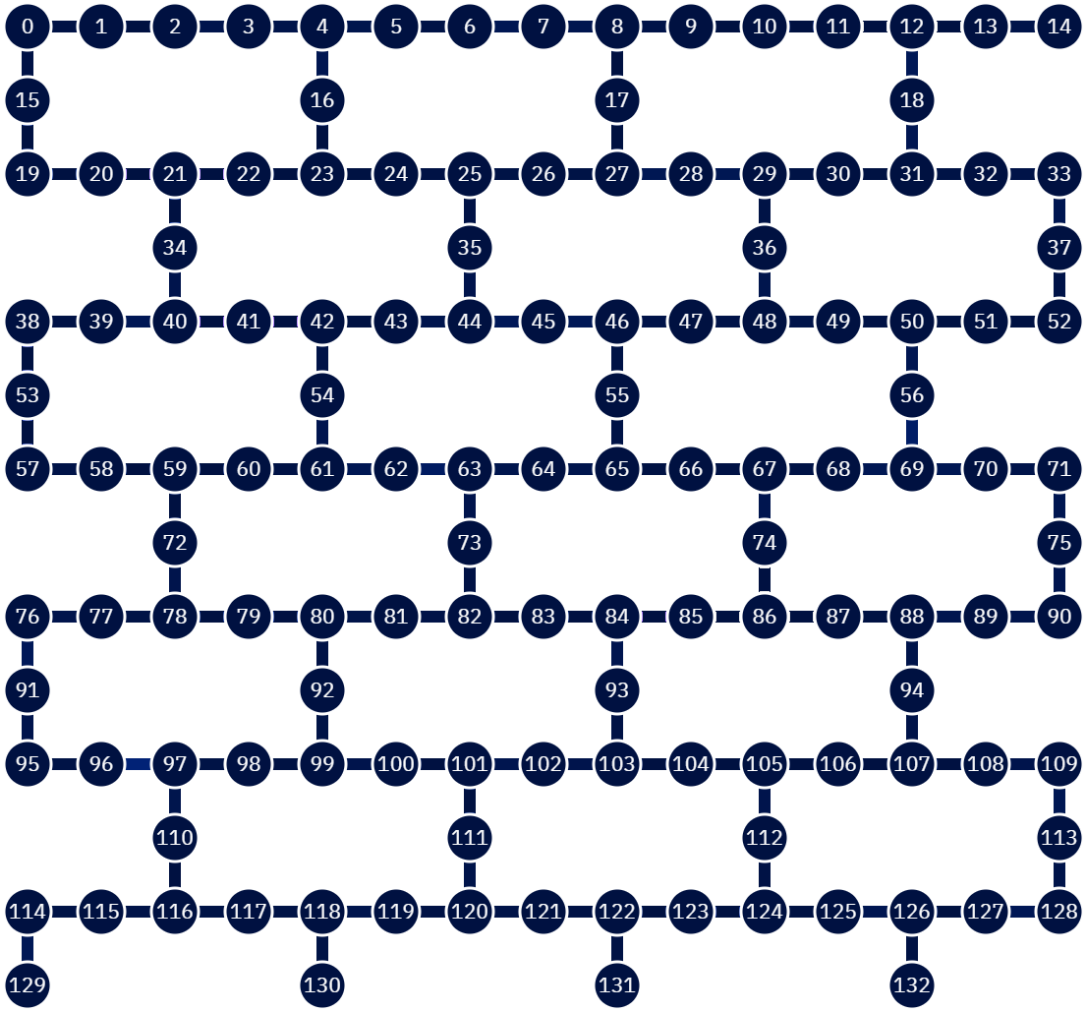


FIG. 4: Qubit distribution map for the backend of `ibm.torino` is demonstrated. Qubit 0 is used for Alice's qubit, and qubit 1 is used for Bob's qubit.

Backend			
	ibm_brussels	ibm_kyiv	ibm_torino
Processor type	Eagle r3	Eagle r3	Heron r1
N_{tot}	127	127	133
Quantum volume	128	128	512
Shots	20000	20000	20000
Readout length (ns)	1500	1244	1560
Qubits used	2	2	2
ECR error	0.01274	0.00612	N/A
CZ error	N/A	N/A	0.00214
Gate time (ns)	660	562	68
CLOPS	220K	30K	210K
Alice's qubit			
Qubit index	0	0	0
T_1 (μs)	370.15	249.70	213.35
T_2 (μs)	105.38	307.57	319.17
Frequency(GHz)	4.898	4.656	N/A
Anharmonicity (GHz)	-0.30830	-0.31106	N/A
Pauli-X error	1.859×10^{-4}	3.073×10^{-4}	3.792×10^{-4}
Readout assignment error	0.0414	0.0035	0.1248
Bob's qubit			
Qubit index	1	1	1
T_1 (μs)	233.54	412.87	291.45
T_2 (μs)	250.55	200.94	194.08
Frequency(GHz)	4.839	4.535	N/A
Anharmonicity (GHz)	N/A	-0.31303	N/A
Pauli-X error	2.487×10^{-4}	1.035×10^{-4}	1.398×10^{-4}
Readout assignment error	0.0177	0.0028	0.0424

TABLE III: The machine properties of the IBM quantum hardware and the parameters used in our experiments are summarized. “Shots” refers to the number of iterations performed for sampling. “CLOPS” refers to the number of circuit layer operations per second, representing how many layers of a circuit the quantum processing unit can execute per unit time. “ECR error” refers to the error rate for the two-qubit ECR gate, employed by the Eagle-type processors, while “CZ error” refers to the error rate for the two-qubit CZ gate, employed by the Heron-type processors. Note that the frequency and anharmonicity information of the qubits for the Heron-type processors is unavailable from the IBM workload source and is therefore not included here.